J Appl Electrochem (2011) 41:415–422
DOI 10.1007/s10800-010-0251-2

ORIGINAL PAPER

The influence of citrate and tartrate on the electrodeposition and surface morphology of Cu–Ni layers

Luisa C. Melo · Pedro de Lima-Neto · Adriana N. Correia

Received: 4 March 2010 / Accepted: 12 December 2010 / Published online: 28 December 2010

Abstract This study examined the influence of citrate and tartrate as complexing agents on the electrodeposition and surface morphology of Cu–Ni layers. The alloys obtained in the tartaric acid and sulphate baths were nobler than those obtained in the citric acid/citrate and citric acid/citrate/tartaric acid media. The results indicated that the complexing medium influences the nobility and the type of mass transport of the alloy formed. The morphology of the electrodeposited Cu–Ni layers changed from a rather porous appearance in the absence of the complexing agents to nodular, cracked mud and cauliflower appearances for the citric acid/sodium citrate/sodium sulphate medium, tartaric acid/sodium sulphate medium and citric acid/sodium citrate/tartaric acid/sodium sulphate medium, respectively. The chemical composition of the Cu–Ni layers revealed the preferential deposition of copper. The ultraviolet–visible spectrophotometry measurements indicated the occurrence of the *d–d* type transition, regardless of the complexing medium employed.

Keywords Electrodeposition · Cu–Ni · Complexing agents · UV–Vis

1 Introduction

The electrodeposition of metal and metal alloys is usually performed in aqueous solutions that contain the metal ions to be deposited on a metal electrode surface, in association with various constituents, such as simple or complex salts. Complex salt solutions contain a component with a complexing action, which acts to ensure the stability of the electroactive species in solution during the deposition process [1–3]. At present, the understanding of the influence of different complexing agents is a much-needed area of research for the development of practical electrodeposited films.

Interest in the electrodeposition of Cu–Ni alloys and their multiple layers is principally due to the various properties of these materials. Their interesting mechanical properties include high tensile strength, malleability and ductility. These alloys also present unique magnetic properties, with Ni displaying ferromagnetism and Cu paramagnetism, as well as good catalytic properties [4]. In recent years, growing interest has focused on the electrodeposition of Cu–Ni alloys in different compositions of electrolytic baths (varying from Cu–5Ni to Cu–64Ni) [5–7], due to their mechanical features and excellent corrosion resistance in aggressive environments. For instance, increasing the nickel ion concentration in the plating solution forms a more corrosion-resistant layer [8]. Cu–Ni alloys, particularly those containing 30–40% Cu, are corrosion-resistant in acidic media, basic media and, most notably, solutions containing chloride (e.g. seawater). This alloy has been used in the construction of seagoing vessels and in heat exchangers cooled with seawater [9–11]. Another application that has motivated the study of Cu–Ni electrodeposition is its use, in powder form, in paints used for protection against the aggressive marine environment [12], as well as in the preparation of nanostructured materials for industrial and electronic applications, such as notebooks and mobile phones [7].

In the formation of the Cu–Ni alloy, the two metals dissolve simultaneously, because they are mutually soluble

L. C. Melo · P. de Lima-Neto · A. N. Correia (✉)
Departamento de Química Analítica e Físico-Química, Universidade Federal do Ceará, Bloco 940, Campus do Pici, Fortaleza-CE 60455-960, Brazil
e-mail: adriana@ufc.br

with each other in the solid state in all compositions, forming solid solution type alloys [13] in which an atom can randomly substitute another in the crystalline lattice. This type of alloy is called a substitutional alloy [14]. The complete solubility can be explained by the fact that both copper and nickel possess the same face-centred crystal cubic structure [15], identical atomic rays, electronegativity and similar valences. The Cu–Ni system is considered isomorphic due to the complete solubility of the two components in liquid and solid states [16].

Due to the difference between the standard electrode potentials of Cu and Ni ($\cong$0.6 V), these ions should be complexed in electrodeposition solutions to facilitate their codeposition [17]. The most traditional complexing agent used in the industrial plating process for Cu is cyanide (cyanide bath) because Cu is easily electrodeposited in the presence of the cyanide anion. However, Ni electrodeposition has low or no current efficiency in the cyanide bath [12]. Moreover, during the last decade, regulations for the protection of the environment and human health have stimulated research to develop environmentally friendly plating solution formulations for use in the electrogalvanic industry. Because the cyanide anion is a strong contaminant in aquatic environments, there has been a push to eliminate cyanide in industrial waste water. Moreover, cyanide is poisonous for human beings because it inhibits the enzyme cytochrome c oxidase by binding to the iron within this protein, thereby preventing the transport of electrons from cytochrome c oxidase to oxygen.

The environmental problems associated with the use of cyanide baths has led to research to find environmentally friendly plating electrolytes that contain non-toxic organic complexing agents, such as organic acids and organic acid-derived anions. The main advantages of these ligands are that they are non-toxic, they are easily obtained and the treatment of the effluent derived from the electrolytes containing these compounds is simpler than that of the effluent derived from the cyanide bath. Some authors [17–20] have suggested that electrolytic solutions containing citrate salts are the most promising for Cu–Ni electrodeposition. The electrodeposits associated with oxalate baths [12], which are characterised by low concentrations of metal species due to the poor solubility of the salts in this medium, tend to be powdery. Tartrate has also been studied as a complexing agent for the electrodeposition of Cu–Sn [21] alloy, and it was shown that the presence of tartrate influenced the layer morphology and decreased energy consumption during the electrodeposition.

Because the presence of these complexing agents influences the surface morphology of the coatings, including the grain size and chemical composition, the aim of this study was to investigate the influence of the citrate, tartrate and citrate/tartrate electrolytes in the electroplating of Cu–Ni alloys on a platinum substrate. Moreover, the electrochemical data on the layer formation was correlated with the electrodeposit morphology.

2 Experimental procedures

Two electrochemical Pyrex® glass cells were used; each cell had a capacity of 60 mL with Teflon® lids containing holes for fitting the electrodes and for the gas inlet/outlets. A platinum disc (99.95%, Heraeus Vectra) working electrode was used with a geometric area of 0.008 cm^2, which was polished prior to use with SiC sandpaper (1500 granulometry). A 0.5 cm^2 auxiliary platinum (99.95%, Heraeus Vectra) electrode was used, while a saturated calomel electrode served as the reference electrode.

Three baths containing equimolar concentrations of the sulphate salts of each metal (0.05 mol L^{-1}), 0.03 mol L^{-1} Na_2SO_4 and the complexing agents were formulated. The citrate bath contained 0.02 mol L^{-1} $H_3C_6H_5O_7$ (citric acid) and 0.2 mol L^{-1} $Na_3C_6H_5O_7.2H_2O$ (sodium citrate), and the tartaric acid bath contained 0.44 mol L^{-1} $C_4H_6O_6$ (tartaric acid); meanwhile, the citrate/tartaric acid bath contained 0.02 mol L^{-1} $H_3C_6H_5O_7$, 0.2 mol L^{-1} $Na_3C_6H_5O_7.2H_2O$ and 0.44 mol L^{-1} $C_4H_6O_6$. A fourth plating solution without the complexing agents was also formulated (sulphate bath). The reagents were of analytical purity, and the solutions were prepared with water purified in a Milli-Q system (Millipore, Inc.). The pH of all solutions was adjusted to 4.8 using 1 mol L^{-1} NaOH or concentrated H_2SO_4, as measured by a Micronal B474 pH meter.

All voltammetric measurements were obtained with a potentiostat (Autolab PGSTAT 30, Metrohm-Eco Chemie) controlled by a personal computer, using GPES version 4.9 software (Metrohm-Eco Chemie) as the data acquisition and treatment program. The rotating disc electrode measurements were carried out using the CTV101 (Radiometer) rotating system with a geometric area of 0.025 cm^2, which was embedded in Teflon®. The morphological characterisation was performed with a Philips XL-30 scanning electron microscope coupled to an X-ray microanalyser. The UV–Vis electron spectra were obtained with a Hewlett-Packard 8453 Diode Array spectrophotometer equipped with a quartz cell (b = 1.0 cm). The electrochemical studies were carried out using cyclic voltammetry (CV), anodic linear sweep voltammetry (ALSV), and rotating disc electrode techniques (RDE). The CV experiments were performed in triplicate at a scan rate of 5 mV s^{-1}. Initially, the electrodeposition behaviour of the alloy only was investigated in a sulphate medium with −0.9 V as the inversion potential. In the experiments involving the use of a rotary platinum disc electrode as the

substrate, rotation speeds of 50–500 rpm were applied. The ALSV experiments were performed in a citric acid/sodium citrate/sodium sulphate medium in the absence of the electroactive species of interest.

For the UV–Vis analyses, a calibration curve was created for the individual metals, using concentrations of 0.010, 0.030, 0.050, 0.075 and 0.100 mol L^{-1}, prepared from solutions of the metal salts dissolved in water. For the Cu–Ni alloy, dilutions to concentrations of 0.01, 0.02, 0.03, 0.04, and 0.05 mol L^{-1} were performed, starting with the solutions of the various electrolytic baths.

A platinum working electrode with an area of 0.5 cm^2 was used to prepare the samples for scanning electron microscopy (SEM) and energy dispersive X-ray (EDX) analyses. The Cu–Ni electrodeposits were obtained by chronoamperometry (CA) in a sulphate medium using a deposition time of 240 s. In the baths containing the complexing agents, the deposition was performed for 1200 s.

All measurements were carried out under ambient conditions (25 ± 2 °C).

3 Results and discussion

3.1 Electrochemical behaviour

Figure 1 shows the potential-current plot of the cathodic scans for the Cu–Ni electrodepositions carried out at 5 mV s^{-1} in all studied plating solutions. This figure shows that the cathodic scan curve, obtained in the absence of the complexing agents, presents three deposition peaks. The first peak, located between 0.13 and −0.05 V (C_1 peak), is not well defined, while the second peak is a well-defined peak that starts around 0.05 V and ends at about −0.15 V (C_2 peak). The third peak, another well-defined peak, starts around −0.53 V and ends around −0.75 V (C_3 peak). The first two peaks are related to the Cu electrodeposition in the sulphate acid solution, where the C_1 peak is related to the Cu underpotential deposition (UPD) and the C_2 peak is associated with the Cu electrodeposition [19]. Meanwhile, the C_3 peak is associated with the Ni electrodeposition. In addition, in the cathodic scan curves for the Cu–Ni electrodeposition in the presence of the complexing agents, the Cu peak potentials are shifted to more negative potential values, and there is no voltammetric peak related to the Ni electrodeposition.

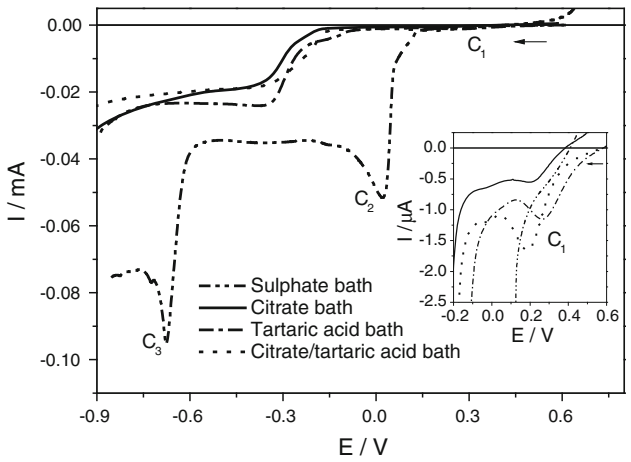

Fig. 1 Cathodic scan for the electrodeposition of Cu–Ni layers on a Pt electrode in different electrolytic solutions with a scan rate of 5 mV s^{-1}

By analysing these results in terms of the values of the initial deposition potential, the following sequence can be established: sodium sulphate medium (∼0.13 V), tartaric acid/sodium sulphate medium (∼−0.10 V), citric acid/sodium citrate/tartaric acid/sodium sulphate medium (∼−0.18 V), and citric acid/sodium citrate/sodium sulphate medium (∼−0.20 V). Because metal ions are Lewis acids, i.e. receptors of electron pairs of a donor ligand, which are the Lewis bases [22], the deposition order of the different systems can be analysed according to the experimental results depicted in Fig. 1 accounting for the stability of the complex in solution. The deposition potential in the citric acid/sodium citrate/sodium sulphate medium is more negative than the deposition potential in the tartaric acid/sodium sulphate medium, due to the metal's electronic density donor effect. The citrate anion has three donor groups, which donate more electrons to the metal and generate greater stability in the complex, thereby hindering its reduction. Moreover, by analysing the chelating effect of the citrate anion, which is greater than that of the tartrate anion, it seems highly likely that the formation of the complexes with citrate is more favourable. A comparison between the citric acid/sodium citrate/sodium sulphate results, and the results obtained in the presence of the mixture of complexants, revealed similar behaviour, as indicated in Fig. 1. One possible explanation may be related to the number of donor sites of the formed complex; more specifically, the complex that was formed had a predominantly citrate nature, which has three donor sites, while tartrate has only two donor sites. These results were confirmed by the ALSV experiments, as shown in Fig. 2, in which the addition of citric acid and sodium citrate led to the formation of a less noble alloy phase.

The hydrodynamic potential-current curves for the electrodeposition of the Ni–Cu layers are shown in Fig. 3. Figure 3a, b show the existence of limiting current plateaus between −0.4 and −0.8 V for the sulphate medium and between −0.5 and −0.8 V in the tartaric acid medium. This indicates that the Cu–Ni electrodeposition in both electrolytes is an electrochemical reaction controlled by

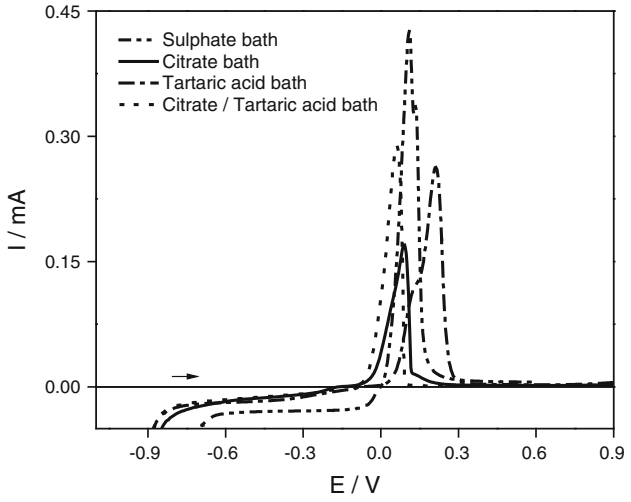

Fig. 2 Anodic linear sweep voltammetry curves for the Cu–Ni layers obtained with the different plating solutions studied

classical diffusion mass transport. For the electrodeposition of the Ni–Cu layers in the citric acid/citrate medium and in the citric acid/citrate/tartaric acid mixture, the formation of diffusional thresholds was not observed (Fig. 3c, d), suggesting that the electrochemical reaction is controlled by a non-classical diffusion mass transport charge or by a mixed mechanism involving both charge transfer and mass transport. These results indicate that the complexing medium influences the mobility and the electrodeposition mechanism of the Cu–Ni layers.

The effect of the addition of the various complexing agents on the current efficiency in the Cu–Ni electrodeposition process is shown in Fig. 4. The current efficiency of the process (η) was calculated from the cyclic voltammograms, and it was defined as the ratio between the anodic charge values, which are related to the dissolution of the Cu–Ni layers, and the cathodic charge, which is associated with the electrodeposition of the Cu–Ni layers. The η values were determined for the different final potentials in the Cu–Ni electrodeposition process.

Figure 4 shows that as the final potential shifts from −0.5 to −0.9 V, all studied plating solutions had high efficiencies. However, a drastic drop in the η values was observed when the final potential was more negative than −0.9 V. This drop is related to the increased competition by the electric charge between the electrochemical reduction of the metal ions and the hydrogen evolution reaction (HER). Rodrigues [20] conducted similar studies in a sulphate medium and obtained current efficiency values of 92% for electrodeposits grown at −0.6 V and 50% for deposits grown at −1.5 V, which clearly indicates the

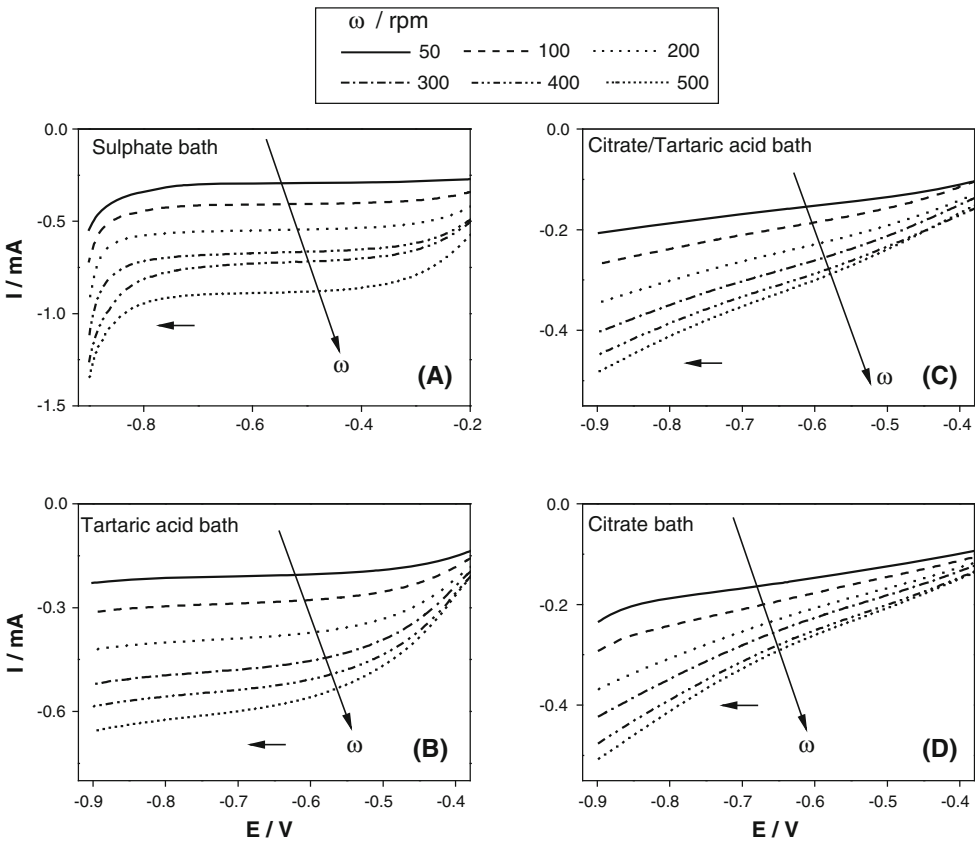

Fig. 3 Hydrodynamic potential-current curves obtained for the electrodeposition of Cu–Ni layers on a rotating Pt electrode in different electrolytic solutions with a scan rate of 5 mV s^{-1} and at different rotating rates

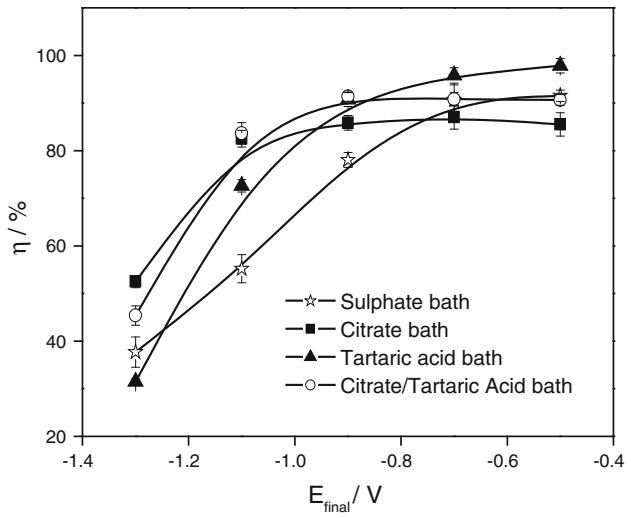

Fig. 4 Dependence of the current efficiency on the final potential for the Cu–Ni layer electrodeposition using the different plating solutions studied

influence of the HER in these studies. No reports were found in the literature on the current efficiency for Cu–Ni electrodeposition in the other systems studied here.

Figure 4 also shows that for final potentials less negative than −0.9 V, the bath containing tartaric acid provided greater efficiency, while the other plating solutions had similar efficiencies. For the final potentials that were more negative than −0.9 V, the citrate and citrate/tartaric acid baths presented higher efficiencies when the final potential was −1.1 V, and the citrate bath had the highest efficiency when the final potential was −1.3 V.

3.2 Physical characterisation

The observed influence of the complexing agents on the morphology of the Cu−Ni layers can be used as a guide for Cu−Ni plating. The electrodeposits used for the physical characterisation were produced by potentiostatic deposition at −1.3 V, which was used to obtain compact coatings of a uniform thickness. In the sulphate bath, a deposition time of 240 s was used, because the absence of complexants causes the cations to rapidly access the electrode surface, which generates low-quality deposits with a strong tendency to flake off. In the other systems, the deposits were obtained after 1200 s because the presence of the complexant in the electrolytic medium generates greater stability of the electroactive species in solution, which causes them to deposit more slowly and forms good quality deposits. The images of these electrodeposits are shown in Fig. 5 a–d, with 10,000× magnification.

The electrodeposits obtained in the sulphate bath (Fig. 5a) were rather porous due to the rapid deposition of

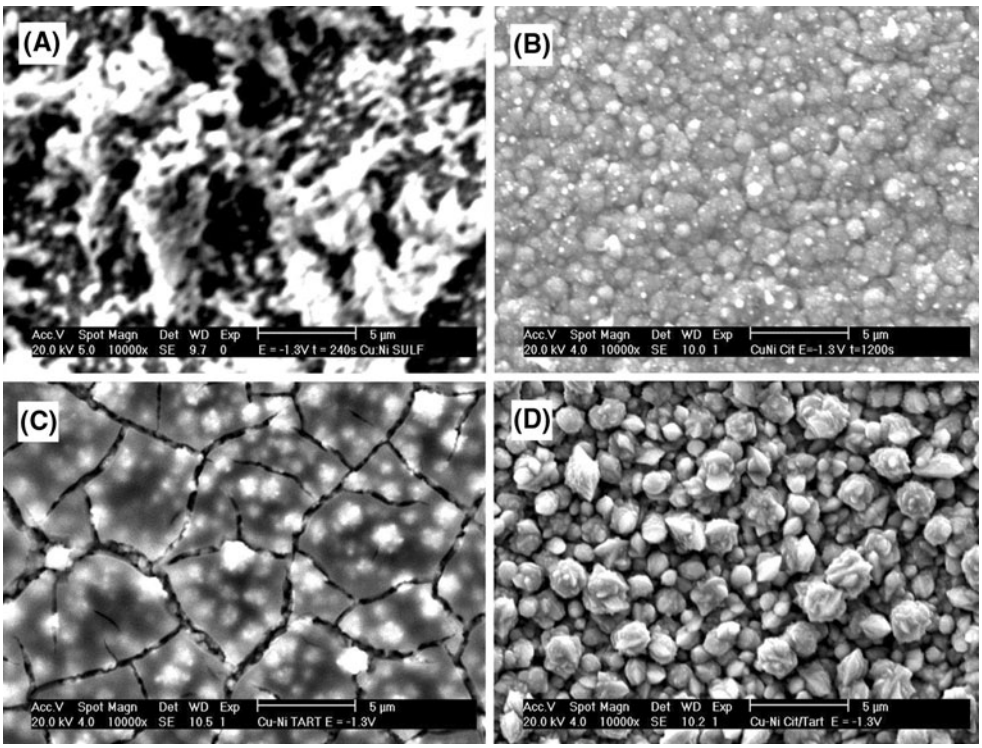

Fig. 5 SEM images of the surface morphology of the Cu–Ni electrodeposits obtained at −1.3 V in the following media: **a** sulphate for 240 s, **b** citric acid/citrate for 1200 s, **c** tartaric acid for 1200 s and **d** citric acid/citrate/tartaric acid for 1200 s

the cations. In the citric acid/sodium citrate/sodium sulphate medium (Fig. 5b), the obtained morphology was nodular with grains of different sizes distributed homogeneously over the entire surface. In the tartaric acid/sodium sulphate medium (Fig. 5c) at −1.3 V, a strong HER was observed, as well as a markedly changed "cracked mud" type morphology, which presented as a nodular inner layer and another surface layer, each with uniform distributions. The mixed medium of citric acid/sodium citrate/tartaric acid/sodium sulphate (Fig. 5d) produced a "cauliflower" type of morphology.

The detection of the different electrodeposit morphology obtained in the tartaric acid/sodium sulphate medium prompted an examination of the dependence of the morphology on the applied deposition potential. Figure 6 a–d shows SEM images of electrodeposits obtained at −0.9, −1.1, −1.3 and −1.5 V for 1200 s using the tartaric acid/sodium sulphate medium. In these images, an abrupt change to the "cracked mud" morphology is clearly visible, indicating this material may be an excellent alternative for electrocatalytic studies under these experimental conditions.

The EDX analyses revealed that the copper content was consistently higher than 80%, as shown in Table 1. This indicates the preferential deposition of copper, especially in the baths containing citrate. It is possible that more stable nickel complexes are formed, thereby hindering the reduction of this metal on the electrode surface.

Table 1 Atomic percentages obtained by EDX for the Cu–Ni electrodeposits at −1.3 V for 240 s (sodium sulphate) and for 1200 s (citric acid/sodium citrate/sodium sulphate, Tartaric acid/sodium sulphate and Citric acid/sodium citrate/tartaric acid/sodium sulphate)

Systems	at.% Cu	at.% Ni
Sodium sulphate	80.5	19.5
Citric acid/sodium citrate/sodium sulphate	98.0	2.0
Tartaric acid/sodium sulphate	83.0	17.0
Citric acid/sodium citrate/tartaric acid/sodium sulphate	96.5	4.4

3.3 UV–Vis experiments

An alteration was observed in the colour of the alloy solutions as a function of the presence of the complexing agents. This prompted a spectroscopic investigation in the visible region, and this alteration may occur because the transition metal coordination compounds involve transitions between the *d* orbitals of the metal.

In general, the spectra of the *d* transition metal compounds comprise a set of weak bands, which are usually wide, have ε_{max} values generally below 50, and are located

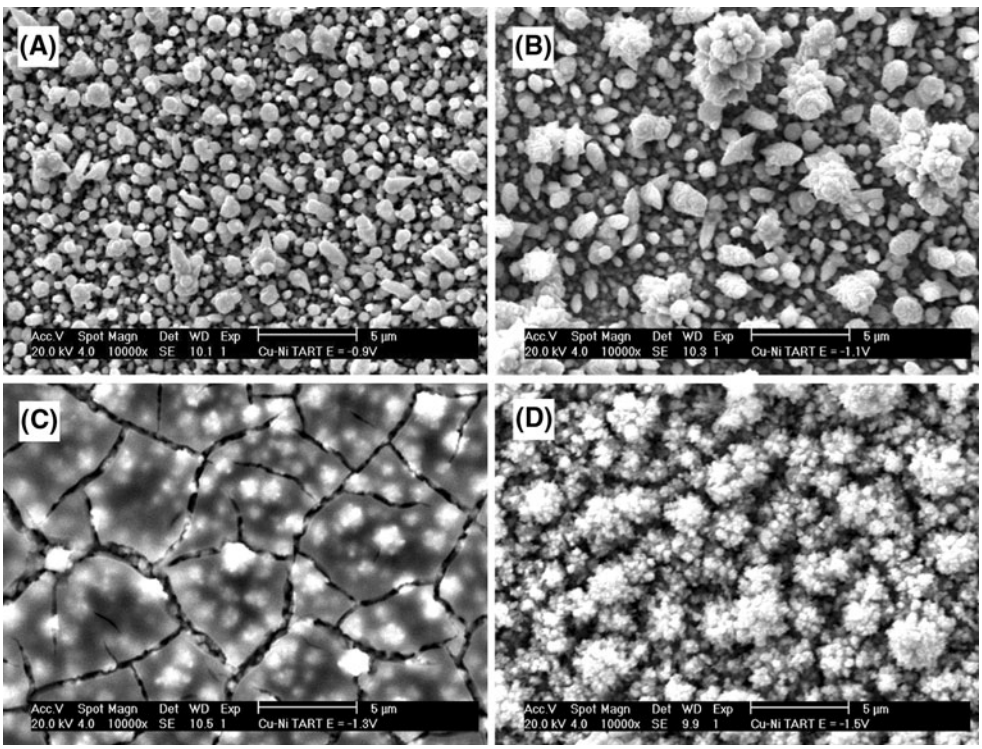

Fig. 6 SEM images of the surface morphology of the Cu–Ni electrodeposits obtained for 1200 s in the tartaric acid medium at **a** −0.9 V, **b** −1.1 V, **c** −1.3 V and **d** −1.5 V

at low wavelengths (350–700 nm). These bands are attributed to the *d-d* transitions and are generally responsible for the colour of the *d* transition metal compounds. The *d-d* transition bands are weak because they are forbidden transitions, according to Laporte's selection rules. More specifically, forbidden transitions are all transitions that involve the redistribution of electrons in a single quantum layer, i.e. transitions between different states of a d^n configuration are not observed [23, 24].

To identify the type of transition occurring in the different electrolytic baths, calibration curves were generated using five different concentrations for both the individual metals and the alloy in the various electrolytic baths. These calibration curves were used to calculate the molar absorptivity (ε). Both the individual metals and the alloy showed low values of ε, suggesting that the transitions were of the *d–d* type, regardless of the complexant used.

Figure 7 shows the superimposed UV–Vis spectra for the equimolar Cu–Ni solutions in different electrolytic baths at a concentration of 0.05 mol L^{-1}. These results suggest that Cu–Ni in the citric acid/citrate bath and in the mixture (citric acid/citrate/tartaric acid) absorb in the visible region close to the copper region, and they present only one well-defined band at approximately 740 nm. However, in the sulphate and tartaric acid baths, absorption occurred in two bands; one band was in the visible region close to the copper transition region, while the other band was close to one of the nickel transitions [25]. A comparison of the results obtained by UV–Vis spectrometry and by EDX indicated that the presence of citric acid/citrate caused the alloy to assume a predominantly copper character.

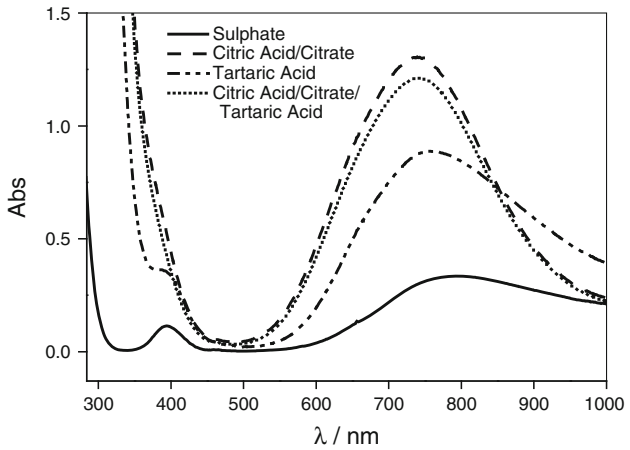

Fig. 7 UV–Vis spectra for equimolar copper and nickel solutions in the sulphate medium under the influence of different complexant agents. The sulphate bath has peaks at $\lambda = 394$ and 796 nm; the citric acid/citrate has a peak at $\lambda = 738$ nm; the tartaric acid has peaks at $\lambda = 386$ and 756 nm; the citric acid/citrate/tartaric acid bath has a peak at $\lambda = 739$ nm

4 Conclusions

The studied complexing agents influenced the electrodeposition and the surface morphologies of the Cu–Ni layers. The Cu–Ni alloy in the tartaric acid bath presented the highest deposition efficiency. However, although the citric acid/citrate medium showed lower deposition efficiency, this efficiency remained constant, while the other systems revealed the influence of the HER at more negative potentials. The alloys obtained in the tartaric acid and sulphate baths were more noble than those obtained in the citric acid/citrate and citric acid/citrate/tartaric acid media. The hydrodynamic experiments showed that Cu–Ni in the sulphate and tartrate media presented diffusional mass transport. The Cu–Ni in the citrate and citrate/tartrate media did not show the formation of diffusional thresholds, suggesting the occurrence of a non-classical diffusion mass transport or a mixed control. These results indicated that the complexing medium influences the mobility and the type of mass transport of the alloy formed.

The morphology of the electrodeposited Cu–Ni layers changed from a rather porous appearance in the absence of the complexing agents to nodular, cracked mud and cauliflower appearances for the citric acid/sodium citrate/sodium sulphate medium, tartaric acid/sodium sulphate medium and citric acid/sodium citrate/tartaric acid/sodium sulphate medium, respectively.

The atomic percent of the alloy's constituents in the different equimolar solutions of Cu–Ni was determined by EDX, which revealed the preferential deposition of copper. The sulphate and tartaric acid baths were richer in nickel, indicating a deposition of about 20%, which dropped to 2 and 4%, in the citrate and citrate/tartrate media, respectively.

In the study of the transitions in the UV–Vis spectra, calibration curves were created for $CuSO_4$, $NiSO_4$ and an equimolar solution of Cu–Ni, which yielded low values of ε. This indicated the occurrence of the *d–d* type transition, regardless of the complexing medium employed.

Acknowledgments The authors wish to thank CNPq, CAPES and FINEP for their financial support of this work.

References

1. Guaus E, Torrent-Burgués J (2005) J Electroanal Chem 575:301
2. Casella IG (2002) J Electroanal Chem 520:119
3. Santana RAC, Prasad S, Santana FSM (2003) Eclética Química 23:1
4. Zhou M, Myung N, Chen X, Rajeshwar K (1995) J Electroanal Chem 398:5
5. Badawy WA, Ismail KM, Fathi AM (2006) Electrochim. Acta 51:4182
6. Ghosh SK, Dey GK, Dusane RO, Grover AK (2006) J Alloys Comp 426:235

7. Baskaran I, Narayanan TS, Stephen A (2006) Mater Lett 60:990
8. Badawy WA, Ismail KM, Fathi AM (2005) J Appl Electrochem 35:879
9. Manzoli A, Santos MC, Bulhões LOS (2006) Surf Coat Technol 200:2990
10. Glibin VP, Kuznetsov BV, Vorobyova TN (2005) J Alloys Comp 386:139
11. Badawy WA, Ismail KM, Fathi AM (2005) Electrochim Acta 50:3603
12. Ponte HA (1994) PhD Thesis, UFSC, Brazil
13. Jovic VD, Jovic BM, Despic AR (1992) J Electroanal Chem 357:357
14. Lee JD (1999) Concise inorganic chemistry. Chapman & Hall, New York
15. Tabakovic I, Riemer S, Sun M, Vasko VA, Kief MT (2005) J Electrochem Soc 152:C851
16. Callister WD Jr (2003) Materials science and engineering: an introduction. Wiley, New Jersey
17. Beltowska-Lehman E, Ozga P (1998) Electrochim Acta 43:617
18. Bonhôte C, Landolt D (1997) Electrochim Acta 42:2407
19. Crousier J, Bimaghra I (1993) J Appl Electrochem 23:775
20. Rodrigues RMB (1991) PhD Thesis, UFSCar, Brazil
21. Carlos IA, Bidoia ED, Pallone EMJA, Almeida MRH, Souza CAC (2002) Surf Coat Technol 157:14
22. Harris DC (2002) Quantitative chemical analysis. Saunders College Publishing, Philadelphia
23. Gushikem Y (2005) Quim Nova 28:153
24. Hutton AE, Elteren JT, Ogorevc B, Smyth MR (2004) Talanta 63:849
25. Felix FS, Barros RCM, Lichtig J, Masini JC (2005) Quim Nova 28:1000